



FEDERAL AVIATION ADMINISTRATION
AAR-100 (Room 907)
800 Independence Avenue, S.W.
Washington, D.C. 20591

Tel: 202-267-8758
Fax: 202-267-5797
william.krebs@faa.gov

July 1st, 2005

From: Vertical Flight Human Factors Program Manager, ATO-P R&D Human Factors

To: Vertical Flight TCRG

Subj: VERTICAL FLIGHT HUMAN FACTORS THIRD QUARTER '05 REPORT

Ref: Vertical flight human factors execution plans (<http://www.hf.faa.gov/vffunded.htm>)

Projects are listed below

- a. Simultaneous Non-interfering Operations - Quantify VFR Navigation Performance.

Naval Postgraduate School (Virtual Model and Oct 2003 Flight Data Analysis Task):

The overarching objective of this program is to assist in the recommendation of the minimum Required Navigation Performance (RNP) value for a VFR helicopter equipped with an IFR GPS. The results of this study combined with the output from another AAR-100's Vertical Flight project entitled "Helicopter SNI helicopter Flight Data" will assist the Federal Aviation Administration flight standards office in determining the minimum RNP value that will be accepted by air traffic office in developing procedures for VFR SNI routes. By correlating human performance data in the simulator to already collected flight data, we will be able to further experiment with new flight patterns towards a decreased minimum RNP value. The purpose of our project is to build and validate the simulation system for further experimentation.

A critical element of our study involves a model of pilot performance as a factor of pilotage cues (e.g. landmarks) and radio communications (e.g. GPS receivers). We need to know if a pilot fixates on landmarks versus GPS output. Do they simply "fly the needle" off of the GPS unit, do they carefully observe visual cues, or is it some mix of both? How does this affect the envelope we can assume they are maintaining, therefore indicating how traffic can be controlled around them? We assume that too much attention to the GPS receiver may adversely affect

pilotage performance, but that the reverse may also be sub-optimal. The study conducted in this program investigates in a virtual environment simulation how traffic density, workload, and weather affect the minimum RNP for a qualified VFR helo pilot equipped with an IFR GPS.

Recent Accomplishments: the primary accomplishments for this period involve attempts to purchase a KLN-89B GPS emulation system, documenting specifications for the simulation system and running additional test subjects.

Panel-mounted GPS Emulation System

As noted in previous reports, a critical portion of recreating the GPS system includes calculating the turn anticipation point and flight guidance for fly-by waypoints. Specifying the system to do this has proved to be relatively straightforward; however, procuring this system has not. While the vendor (Frasca International) originally did not anticipate difficulty, the unusual nature of the purchase has significantly delayed the process. The primary difficulty arose from expiration of and ensuing discussion concerning the Non-Disclosure Agreement between Frasca and the GPS manufacturer (Honeywell). Honeywell’s concerns were based on losing potential revenue sources by making the algorithm widely available. Their intent was to maximize revenue from training applications that used their GPS systems. This conflict was resolved in late June. Unfortunately, during this time approval to use the most expedient contracting vehicle to make the purchase (Open Market Corridor) was rescinded by DoD. Purchase requests using a new contract vehicle have been processed by NPS. The current worst-case delivery date is 21 July. Since this date is uncomfortably close to the date for analyzed data, in depth discussion of the scope of work, likely time frame and alternatives is ongoing. Estimated completion time between receiving the equipment and analyzing the data is between one and three weeks.

Documentation for Recreating Simulation System

We have started the process of documenting the simulation system. A preliminary list of system goals, operating environment constraints, component characteristics and lessons learned is available to the public. If someone wants to replicate the system, the major hardware components for the visual display system and their cost is listed in Table 1.

Qty	Description	Unit Cost	Total Cost
3	Custom Draper RPS Complete NTSC format 120" with IRUS screen	\$15,833.33	\$47,500.00
3	Christie Vivid LX37 #38-VIV211-02	\$4,759.85	\$14,279.55
3	Christie Lens 0.8:1 Fixed #38-809049-01	\$2,219.00	\$6,657.00
1	RealSims FasTrac OH58A Instrument Console	\$3,750.00	\$3,750.00
1	Frasca KLN-89B emulation system	\$15,000.00	\$15,000.00
2	EGT/Fuel Flow Indicator, Part 2616	\$191.87	\$383.74
2	Fuel Indicator Left/Right, Part 2609	\$191.87	\$383.74
2	Oil Temp & Press Indicator, Part 2623	\$191.87	\$383.74
1	Suction Gauge/Ammeter Part 2630	\$191.87	\$191.87

1	KX155A/165A NAV/COM part 2708	\$512.08	\$512.08
1	Front Ring Small partno.: 1398	\$10.37	\$10.37
1	Central Control Unit	\$195.00	\$195.00
1	ADF Indicator	\$169.00	\$169.00
1	Attitude Indicator	\$169.00	\$169.00
1	VOR 2 Indicator	\$189.00	\$189.00
1	Airspeed Indicator	\$128.00	\$128.00
1	Turn Coordinator	\$169.00	\$169.00
1	Vertical Speed Indicator	\$128.00	\$128.00
1	Digital Clock	\$89.75	\$89.75
1	Altimeter (Inches Scale)	\$179.00	\$179.00
1	Wet Compass controlled by CCU	\$269.50	\$269.50
1	SimKits Heading Indicator, Part # 2579	\$246.15	\$246.15
			\$90,983.49

Table 1. Visual Display Equipment for Virtual Tullahoma

Results of Additional Data Collection

An additional four test subject trials have been completed. Pilot performance and debrief comments indicate that the changes to the simulated environment incorporated based on feedback from previous data collection trials were effective. Each of the four subjects agreed that the preflight introduction and practice adequately prepared them to use the GPS and navigate the PVFR route in the virtual environment. Additionally, pilots generally found the workload and navigation task in the simulator were roughly the same as in the aircraft. The primary area of difficulty was a result of the GPS emulation system: without an accurate turn-anticipation function, pilot's radius of turn occasionally took them well outside the prescribed flight path. This can be seen in the representative flight path for subjects one and three shown in Figure 1 and Figure 2. Pilots tended to overshoot waypoints 2, 5 and 9.

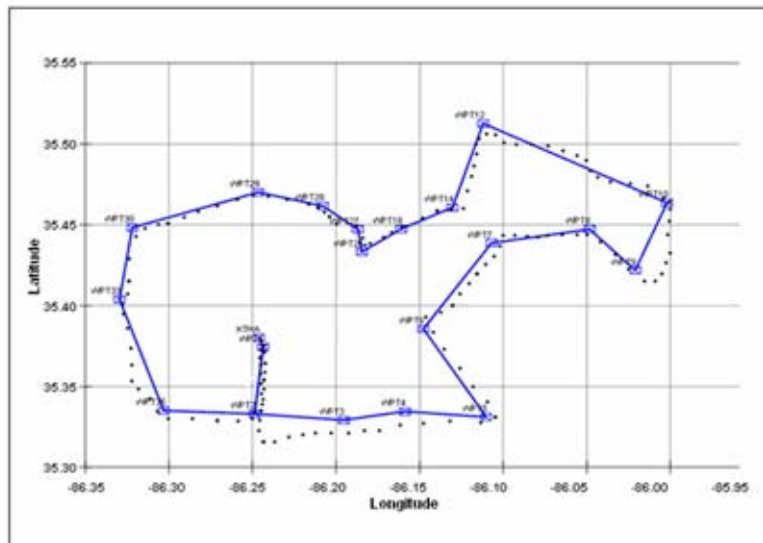


Figure 1. Subject One Flight Path

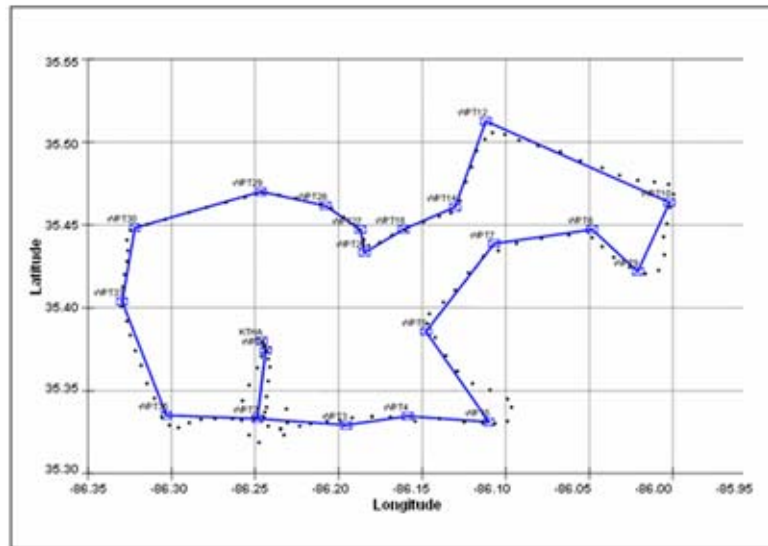


Figure 2. Subject Three Flight Path

Without the turn anticipation feature of the GPS, turns greater than 90 degrees led to the most significant deviations from course. The nature of these waypoints and pilot's performance may suggest guidelines for selecting visual cues for turns greater than 90 degrees and areas of future study. At waypoints defined primarily by GPS coordinates, predicted performance matched pilot performance. Because the primary cue for starting a turn to stay on track was GPS and the GPS did not account for radius of turn the actual aircraft track would be expected to overshoot the ideal track. This condition applies to waypoint two where three of four subjects overshoot the track significantly.

Of the other four waypoints with turns greater than 90 degrees, the greatest errors occurred at waypoints 5 and 9. Navigation errors at waypoints 12 and 26 were less than those at 5 and 9. This could be due in part to the nature of the visual cues. Checkpoints 5 and 9 both involve recognizing and starting a turn in time to parallel a feature that is nearly perpendicular to the flight path. At waypoints 12 and 26 pilots have some advanced cueing. Waypoint 12 is defined as the intersection of a highway that parallels the route segment and power lines. The power lines are clearly visible well ahead of the waypoint. They run parallel and slightly offset from the route approximately half a mile prior to the waypoint. The route to waypoint 26 follows a waterway. Waypoint 26 is defined by a sharp bend in this waterway. One could also attribute pilot's performance at these waypoints to a learning effect. Pilot's seemed to have greater navigation errors on the turns over 90 degrees earlier in the flight. Analysis of eye track information or future study may be helpful for providing guidelines for selecting cues that allow adequate time to recognize the new course and account for radius of turn.

NASA Ames (Eye Tracking Analyses)

The primary activity for this period has been the development of new procedures for analyzing the eye images collected during the October 2003 flight tests. A number of new software components have been developed: first, we have developed a system for grouping the images based on visual similarity. Figure 1 (below) shows a set of images extracted from one of the daytime runs which spans the entire data set; after choosing a threshold (based on correlation), the entire recording is scanned, with the goal of selecting a set of exemplar images such that each image in the set differs from each of the other images by at least the threshold distance, and all other images are within the threshold distance of at least one of the exemplar images.

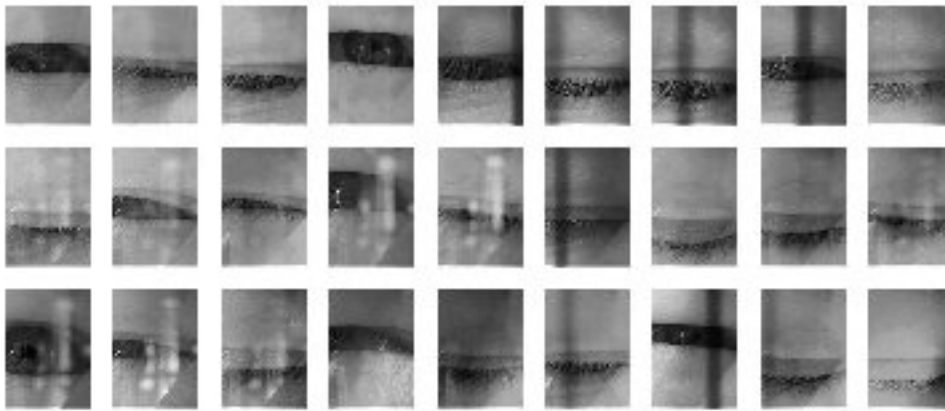


Figure 1: Set of exemplar images determined from a typical day flight recording.

Figure 2 shows a two-dimension cartoon illustrating the process: the filled disks numbered 1, 2, and 3 represent the first three exemplar images, and the circles represent the threshold difference. The images are processed in temporal sequence; a new exemplar is created when an image is encountered whose distance from all of the existing exemplars exceeds the threshold. After the list of exemplars has been determined, a second pass is performed over the data to determine which of the exemplar images are the nearest-neighbor to each input image. Each of these neighborhoods may be processed recursively with a smaller threshold value. Ultimately, we have groups of images all having similar appearance, which may be processed in a similar manner.

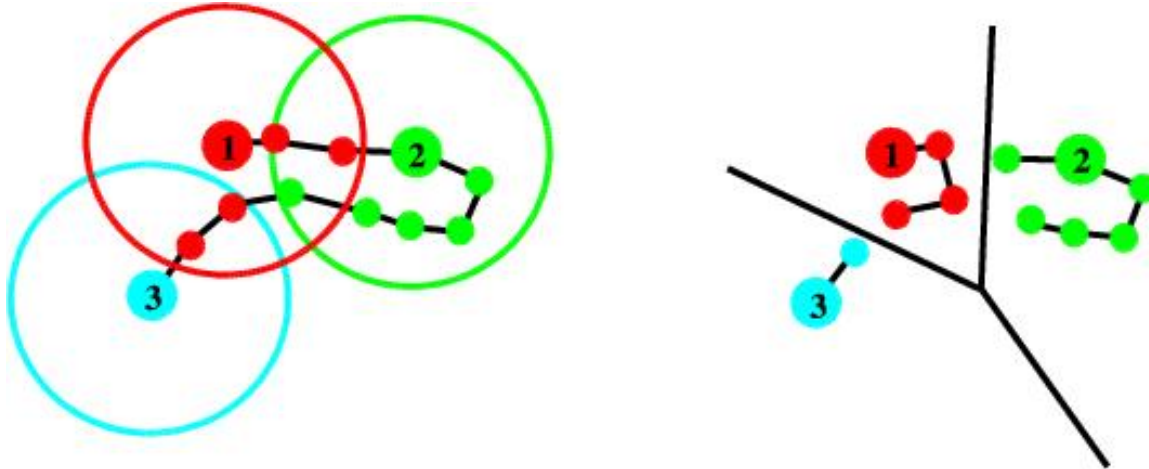


Figure 2: Two-dimensional cartoon illustrating the computation of image neighborhoods: the first image (represented by the red disk labeled “1”) is chosen as the first exemplar, subsequent images are associated with it as long as their distance is within a preset threshold. When an image exceeds the threshold distance from the current exemplar, it is checked against all other exemplars, and if there is no exemplar within the threshold distance a new exemplar is created. After a spanning set of exemplars has been computed, an second pass is performed to determine the nearest exemplar to each image (illustrated on the right).

Sets of exemplar images have been computed for each of the 15 runs. We are in the process of hand-labeling the first-level exemplars; two types of labeling are being performed. The first type of labeling involves locating the upper and lower eyelid margin, the limbus (outer iris boundary), the pupil (inner iris boundary), and the reflections of the LED illuminators. The second type of labeling involves fitting a geometrical model of the pupil and limbus to the image. Examples of pupil/limbus labeling are shown in figure 3. The ellipses drawn over the images represent different rotations of a rigid three-dimensional model of the eye; because the model pose is specified directly in degrees, no angular calibration is required; the calibration sequences will be used only to determine the absolute offset.

Planned work for the fourth quarter includes completion of the labeling and integrating the results with the head-tracking results. Additional disk drives have been purchased to allow installation of an additional web server to host the raw and processed data. A new research assistant was hired in June who is doing the bulk of the hand-labeling. Progress on the project has been hampered by the fact that NASA's Human Measurement and Performance project (which had been supporting the infrastructure and basic technology development used in the project) was cut in FY05 due to congressional earmarks. Nevertheless it is hoped that processing of the data from the 2003 flight tests will be completed by the end of the summer. The tools developed in this effort should make processing of additional data currently being collected at the Naval Postgraduate School relatively straightforward.

NASA Ames effort is cost shared with the FAA. In coordination with program sponsor, new milestones have been established. Final report will be delivered at the end of FY06Q1.

b. Lowering GA Accidents in Low Visibility: UAV See-and-Avoid Requirements

The goal of this project is to assess the feasibility of using the Spatial Standard Observer, or derivatives, to compute N50 values for target image sets. Currently N50 values are obtained empirically, through an expensive and time consuming psychophysical experiment using human observers. Because the SSO attempts to model human image discrimination, it offers the possibility of replacing human observers with computer calculations. Further information on project goals is available in the project plan

http://www.hf.faa.gov/docs/508/docs/VFsee_avoid.pdf.

The initial effort in this project has been to attempt to simulate the results of a recent psychophysical experiment that estimated N50 for a set of military vehicles.

We received two sets of ARF images from Eddie Jacobs, Performance Modeling Team, US Army CECOM NVESD. The first set consists of visible, IR, and MWR images of military vehicles. The second consists of various hand-held objects (cell phone, knife, gun, etc.). We have initially analyzed the visible military vehicle set. The source images consisted of 144 digital images, of 12 “objects” in 12 “aspects.” An illustration of two of the objects and three of the aspects are shown in Figure 3. Each object is a particular military vehicle, and each aspect is a view of that vehicle. The viewpoints are approximately the same from object to object.



Figure 3. Example images. Two objects and three aspects are shown.

In the psychophysical experiment, the images were subjected to six levels of Gaussian blur. Identification experiments using trained human observers were run separately on each level of blur.

The first model we have considered is a simple image classification machine operating on the basis of a normalized correlation matching rule. This model

computes a set of N discriminant functions, where N is the number of possible images (in this case, $N = 144$). One discriminant corresponds to each candidate image, and the model selects the image with the largest discriminant.

The matching is assumed to occur in a “neural image” space, which is reached by transforming the image. The transformation consists of a conversion to contrast and a filtering by the SSO CSF. The templates consist of the transformed images. At present we are not including masking in the model.

The normalized correlation model leads to simple Monte Carlo simulation of proportions correct in an identification experiment (it can also generate confusion matrices). We compute both percent correct image identification and correct object identification. The performance of the model is controlled by a single parameter: the standard deviation of the “neural noise” added to the sample neural image. In Figure 4, we plot the percent correct for image identification and vehicle identification for images blurred by 30 pixels. As expected, increasing noise reduces performance.

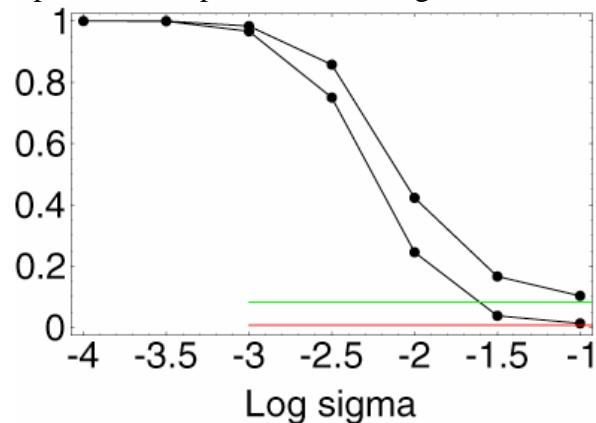


Figure 4. Percent correct image (lower curve) and object (upper curve) identification for various levels of the noise standard deviation. These results are for blur scale = 30 pixels. Green and red lines indicate guessing performance.

The results for image identification can also be plotted as a function of blur scale, as shown in Figure 5. Each curve is for a different noise sigma. The figure also includes (red curve) the data from the human observers. No attempt has been made at this point to find the best fitting value of noise sigma, but it is clear that a value of around 2.25 yields a rough approximation to the human data.

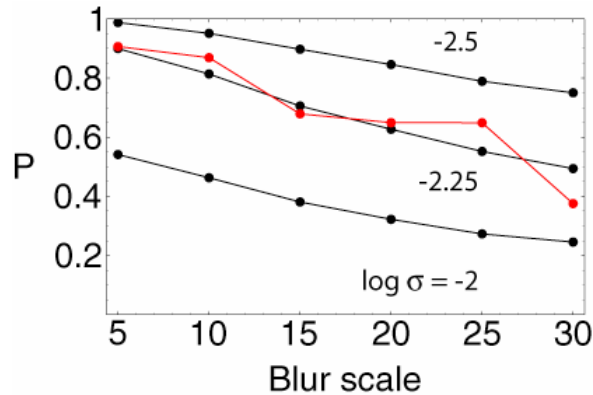


Figure 5. Simulated percent correct identification as a function of blur scale for several different values of neural noise.

These results show the feasibility of simulating human target identification data using an SSO-based image identification model. However, this should not distract from potential difficulties. In particular, caution must be observed in application of an image identification model to object identification experiments. We will consider this issue further in future work.

Additional activities

- Developed software to read images into Mathematica modeling environment.
- Analyzed report that describes the psychophysical experiment. Clarified details of images, stimulus presentation, display calibration, data collection and data analysis.
- Met with Eddie Jacobs, US Army RDECOM CERDEC NVESD, Fort Belvoir, VA, and Steve Murrill, Army Research Laboratory, Adelphi, MD to review details of psychophysical experiment and to discuss current progress (6/24/05).
- The researcher continued literature analysis. Papers read and analyzed: Driggers, R. G., Vollmerhausen, R., Devitt, N., Olson, J., & O'Connor, J. Fifty-percent probability of identification (N50) comparison for targets in the visible and infrared spectra: US Army Night Vision and Electronic Sensors Division (NVESD).
- Researcher finalized journal article describing the model underlying the Spatial Standard Observer:
Watson, A. B., & Ahumada, A. J., Jr. (in press). A standard model for foveal detection of spatial contrast. *Journal of Vision*.
- Researcher began draft of paper describing model of letter acuity based on Spatial Standard Observer.

Planned activities for next quarter

- Continue development of Mathematica software for image identification.
- More detailed simulations of current model
- Test other matching rules, templates, and sources of noise
- Apply model to infrared images, compare to visible

- Consider deterministic predictions of performance.

This effort is cost shared with NASA Ames

William K. Krebs, Ph.D.